Journal of Loss Prevention in the Process Industries 101 (2026) 105966

Contents lists available at ScienceDirect

Journal of Loss Prevention in the Process Industries

journal homepage: www.elsevier.com/locate/jlp

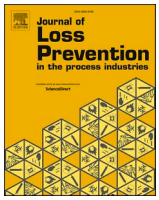

Fire behaviour of biopolymer wet in flammable solvent

Benedetta A. De Liso, Gianmaria Pio, Ernesto Salzano *

Department of Civil, Chemical, Environmental, and Materials Engineering, University of Bologna, Bologna, 40131, Italy

ARTICLE INFO

Keywords:
Thermal degradation
Solid-liquid mixtures
Cone calorimeter
Polymers

ABSTRACT

Several industrial processes deal with solid-liquid hybrid mixtures composed of flammable or combustible species, posing concerns about their behaviour once exposed to undesired conditions, including fires. However, a poor understanding of the safety aspects and possible synergistic effects of the species constituting the mixtures has been gained. This is particularly relevant for polymer production, where innovative materials are continuously introduced. For these reasons, this work presents an innovative and comprehensive methodology for the evaluation of microscopic and macroscopic aspects ruling the fire-behaviour of solid-liquid mixtures of carbon-based substances. Lab-scale thermal analysis (Differential Scanning Calorimetry, DSC, Thermogravimetric Analysis TGA, and TGA coupled with Mass Spectroscopy, TG-MS) and bench-scale thermal oxidative analysis (cone calorimetry) were carried out. Isothermal tests, coupled with mass spectroscopy analyses, have elucidated the chain of events occurring under pyrolysis conditions, whereas fire tests have shed light on the ignitability and the overall kinetics and exothermicity. The proposed approach was applied to the cases of Polyhydroxybutyrate (PHB), Poly(3-hydroxybutyrate-co-3-hydroxyvalerate) (PHBV), and PHBV-toluene mixtures. The vapour production from liquefied polymer was identified as the rate-determining and crotonic acid was identified as the species ruling the gas-phase reactivity of the polymer. Although two distinguishable behaviours were observed during the degradation of wet polymers, each of them attributable to a pure compound, toluene-polymers interactions were identified, allowing for the realisation of advanced models suitable for an optimised design of industrial processes involving wet polymers.

1. Introduction

The utilisation of hybrid mixtures involving carbon-based and potentially flammable solids and liquids is largely used, especially in the polymer industry. Indeed, within the polymer life cycle, solvents are adopted for synthesis, as coagulation agents to facilitate polymeric precipitation in the production phase, and as a dissolution agent, either in the production phase or during the chemical recycling of plastics. The suspension polymerisation (e.g., for the production of High-Density Polyethylene, HDPE, or Poly Vinyl Chloride, PVC) and the solution polymerisation (e.g., for Poly Methyl Methacrylate, PMMA) typically use common hydrocarbons, including pentane, hexane, toluene, or decane. The production of biopolymers (e.g., polyhydroxybutyrate, PHB and poly(3-hydroxybutyrate-co-3-hydroxyvalerate), PHBV) typically involves flammable solvents for gelation processes (Pich et al., 2006b) and extractions from organic materials (Vermeer et al., 2022; De Liso et al., 2024). Dealing with hybrid systems consisting of liquid and solid species requires dedicated analyses and characterisation for a proper design of the processes (De Liso et al., 2025). In this light, recent studies have been focused on the evaluation of physical properties (e.g., solubility) of PHBV in liquid solvents (Abate et al., 2024). Besides, chemical recycling has become an essential approach to tackling plastic waste challenges (Ragaert et al., 2017). Among the solvents used for dissolution, aromatic substances, with specific reference to toluene, outperformed all the other solvents in solubility (Tsampanakis and Orbaek White, 2021). In this sense, the coexistence of flammable liquids and solids can have synergistic effects, raising concerns about the safety performance of processes that employ hybrid mixtures. Nevertheless, a poor understanding has been achieved in terms of flame characterisation and degradation processes. Given the inherent complexity of these multi-phase systems (liquid permeation, enhanced heat transfer coefficient between liquid and solid, mass transfer capillarity effects, and micro-scale structures), an in-depth analysis of the kinetic and ruling phenomena of thermal degradation and fire behaviour is not evident in

This article is part of a special issue entitled: Selected articles of the ISFEH11 published in Journal of Loss Prevention in the Process Industries.

* Corresponding author.
E-mail address: ernesto.salzano@unibo.it (E. Salzano).

https://doi.org/10.1016/j.jlp.2026.105966
Received 8 September 2025; Received in revised form 11 December 2025; Accepted 5 February 2026
Available online 6 February 2026

the current literature (Zhang and Chen, 2022). Within this scope, different experimental techniques can be employed to determine the microscopic and macroscopic behaviour of solid-liquid mixtures exposed to an external heat source. Among the others, Differential Scanning Calorimetry (DSC) and Thermogravimetric Analysis (TGA) are two common technologies used to experimentally evaluate phenomena involving a change in the heat capacity and thermal capacity of the material across a wide temperature range and to investigate thermal and thermo-oxidative stability (Hong et al., 2013). More recently, the Cone Calorimeter (CC) has been used to characterise the thermal stability and degradation mechanisms at the bench scale, integrating results from traditional calorimetry techniques (Girods et al., 2011). Previous studies have suggested that the cone calorimeter is the most suitable solution for the direct measurement of the mass loss rate, together with the heat release rate and time to ignition of species in a condensed phase, whereas classical calorimetric analyses are suggested for the evaluation of micro-kinetic aspects (Patel and Wang, 2016; Wu et al., 2023).

In this work, an innovative procedure to determine the microscopic and macroscopic aspects relevant for the safety characterisation of hybrid mixtures is proposed. The main features of this methodology were discussed in the view of a case study involving PHB, PHBV, and PHBV-toluene mixtures. The investigated materials were tested by lab-scale thermal analysis (TGA and DSC) and bench-scale thermal oxidative analysis (CC). The collected data were utilised to identify the most relevant phenomena and the rate-determining steps of the degradation mechanism, as well as to quantify the most relevant parameters describing the ignitability and flame behaviour of the investigated mixtures.

2. Methodology

2.1. Overview

For the sake of safety considerations, a complete understanding of the phenomenological aspects involving the degradation of solid-liquid mixtures exposed to fire conditions is paramount, as well as the determination of macroscopic, empirically based parameters. Within this scope, this work presents an innovative multi-step methodology combining experimental and numerical analyses for a comprehensive characterisation of fire-related scenarios, as schematized in Fig. 1 and detailed in the following sections.

2.2. Selection of solid-liquid mixtures of interest

The main features of the proposed approach were tested for a case study consisting of PHB, PHBV, and PHBV-toluene mixtures. More specifically, polyhydroxybutyrate (PHB, ENMAT™ Y3000P) and poly(3-hydroxybutyrate-co-3-hydroxyvalerate) (PHBV, ENMAT™ Y1000P) were tested either in dry conditions or wet with toluene (Sigma Aldrich, purity $\geq$99.7 $\%_v$). High-purity polymers were adopted for this scope to minimise the effects of composition. Additional information on the mechanical and chemical characterisation of the investigated materials can be found in the dedicated literature (Koller and Mukherjee, 2022; Srubar et al., 2012). Wet polymers having initial mass ratios of PHBV to toluene within the range of 0.66 – 3 were studied. The effects of mixing were evaluated by repeating the small scale experiments at different contact times, up to 250 h.

2.3. Determination of the possible chain of events

The characterisation of the decomposition pathways of hybrid mixtures exposed to an oxidative environment and an external heat flux requires the identification of the most relevant phenomena ruling the heterogeneous system and the utilisation of suitable models accounting for each of them. Indeed, considering the heterogeneous nature of the investigated systems, the overall reaction process can be intended as a combination of phenomena occurring in series or parallel. More specifically, heterogeneous oxidation, solid liquefaction, liquid evaporation, volatilisation, cracking, and homogeneous oxidation can play a relevant role, as schematized in Fig. 2.

Considering the fluid dynamic regimes and the limited movement of solid particles for the systems under investigation, an oxygen diffusion-

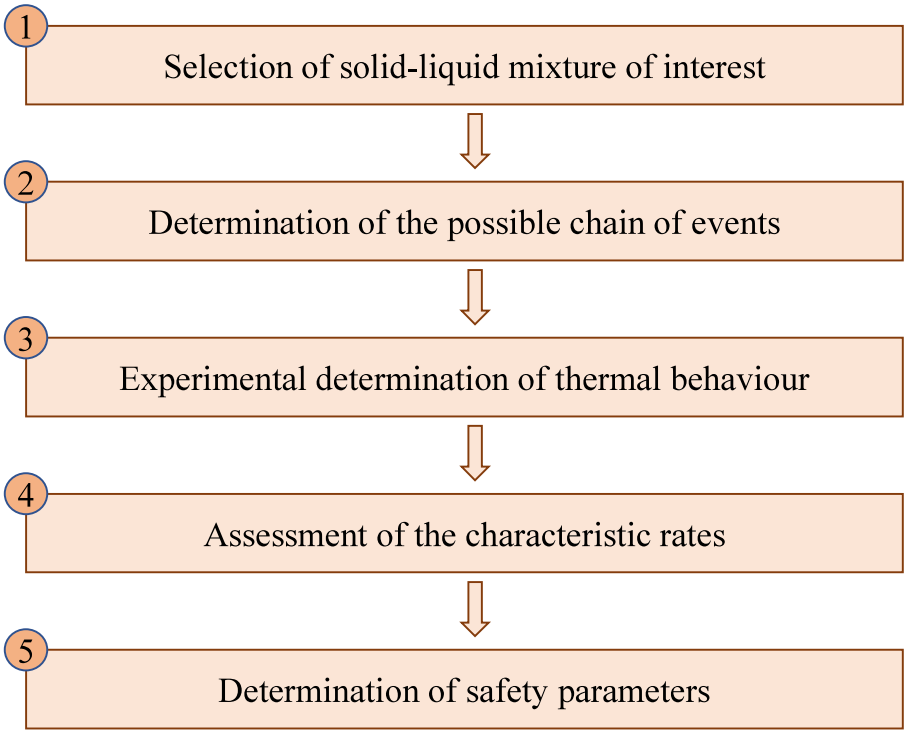

Fig. 1. Schematic representation of the methodology developed in this work for the characterisation of solid-liquid mixtures.

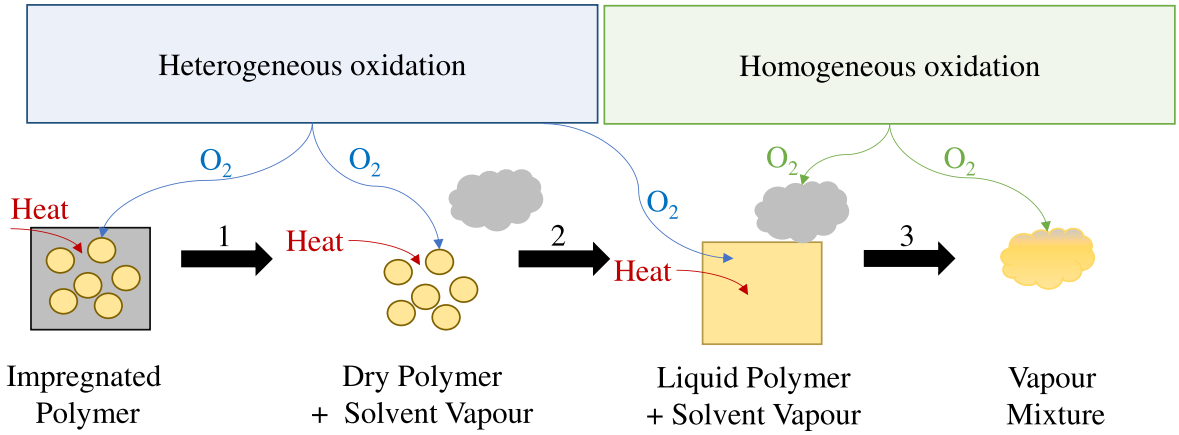

Fig. 2. Schematic representation of a possible degradation pathway for wet polymers exposed to an external heat flux under an oxidative environment.

limited regime can be expected for the heterogeneous oxidation. Following the reported chain of events, this phenomenon appears to be in parallel with faster alternatives. Hence, heterogeneous oxidation was neglected in the kinetic model under development. Therefore, the first step can be assumed to consist of the evaporation of liquid solvent and the heating of solid particles. Indeed, the boiling temperature of solvents is typically considerably lower than the melting temperature of carbonaceous particles. Under these hypotheses, gas-phase reactions involving solvent-based vapours and the liquefaction of dry polymers can be considered as the second stage, whereas the production of vapour mixtures containing species based on solvent and polymer degradation can be assumed as the third stage. Within this stage, different alternative pathways can describe the degradation of dry polymers, e.g., liquid cracking of polymers to form light species or non-reactive evaporation. Therefore, a specific analysis of the characteristic rate for each step is necessary.

2.4. Experimental determination of thermal behaviour

To evaluate the physical and chemical transformations characterising dry polymers, preliminary lab-scale thermal analyses are recommended together with an integrated bench-scale testing. To this scope, DSC, TGA, and the CC were employed in this work. For all the thermal techniques employed in this work, the samples were always tested in their original form as pellets, without grinding or further physical modification. Regardless of the technique, each condition was tested 3 times to guarantee the repeatability of the data and robust analysis. For the sake of simplicity, the average values were reported exclusively since variations within ±5% were observed.

DSC measurements were performed in a nitrogen atmosphere utilising a TA Instrument Q2000. Considering the expected thermal behaviour of the investigated species, runs were carried out at a maximum temperature of 360 °C to ensure the accurate observation of all the phenomena of concern for this analysis and to avoid exceeding the maximum operable temperature. Approximately 0.02–0.04 g of pellets were placed in standard aluminium crucibles (40 μL) equipped with pierced lids to allow venting of volatile decomposition products. Heat flow was recorded as a function of temperature.

TGA was performed by a TA Instruments Q500 using both isothermal and temperature-controlled tests under a nitrogen atmosphere. More specifically, after a fast-heating phase, different tests were carried out at a given constant temperature within the range of 200 – 500 °C. Once temperature-controlled tests are considered, the adopted heating rates were 10, 25, and 40 °C/min, whereas the maximum temperature was set to 600 °C according to the expected relevant temperatures reported in the current literature (Lee et al., 2001). In both cases, a nitrogen flow rate of 100 mL/min was used. Mass loss was recorded with respect to temperature, and Derivative Thermogravimetry (DTG) curves (dm/dT) were obtained by numerical differentiation of the raw TGA signal. Thermal gravimetric mass spectrometry (TGA-MS) was performed by a TA instrument SDT Q600, which features an electron ionisation source and a Faraday detector, to identify the species produced during the third phase of the postulated mechanism. During the analysis, the gaseous degradation products released from the sample are ionised and detected according to their mass-to-charge ratio (m/z), enabling the qualitative identification of the volatile species evolving throughout the decomposition process. The samples were heated (10 °C/min) under a nitrogen flow of 100 mL/min, reaching a maximum temperature of 600 °C. Based on the key intermediates and final products identified at this stage, the rate of gas-phase oxidation was quantified in terms of fundamental laminar burning velocity. Data available in the current literature can be considered when available. Alternatively, comprehensive, detailed kinetic mechanisms (e.g., KIBO, Gri-Mech, LLNL/NUIG (Bugler et al., 2015; Fairweather and Woolley, 2004; Pio et al., 2022)) can be employed for their assessment by using a dedicated script available in Cantera, an open-source code dedicated to kinetic analysis, assuming a one-dimensional, adiabatic, and premixed reactor. Additional information on the numerical setup can be found elsewhere (De Liso et al., 2023).

A cone calorimeter was adopted (Fig. 3) to characterise the heterogeneous mechanisms on a bench scale (Schinazi et al., 2022). The tests were carried out by exposing materials having a rectangular cuboid shape with sides of 10 cm × 10 cm and an initial thickness of 1 cm to different heat fluxes within the range of 7 – 50 kW/m^2. The heat flux was produced by a conical-shaped resistance located 2.5 cm from the sample. CC tests were carried out based on the geometrical configuration and the protocol provided by the standards ASTM E1354:2023 and ISO 5660-1:2019 (ASTM E1354, 2023 ISO 5660, 2019). Standard cone sample pans were used, following the conventional preparation procedure: each sample was prepared by placing a sheet of aluminium foil in the pan, upon which the specimen was carefully arranged before testing. Polymer/solvent mixtures were prepared by combining polymer pellets with the liquid solvent, stirring the mixture to ensure homogeneous wetting, and placing the mixture directly into the standard pan. No additional containment structures or special accommodations were required, and the tests were carried out in accordance with common practice for liquid systems (DiDomizio et al., 2021). A continuous external spark of 10 kV was provided after a stabilisation time until a stable flame was not already present. The mass of the sample and the mass loss rate (*MLR*) were continuously measured by means of a load cell. The MLR reported in this work was obtained by applying a minimal Savitzky–Golay smoothing filter (second-order polynomial, 7-point window) to the measured data to reduce high-frequency noise without affecting the physical trends of the signal. Temperature and composition

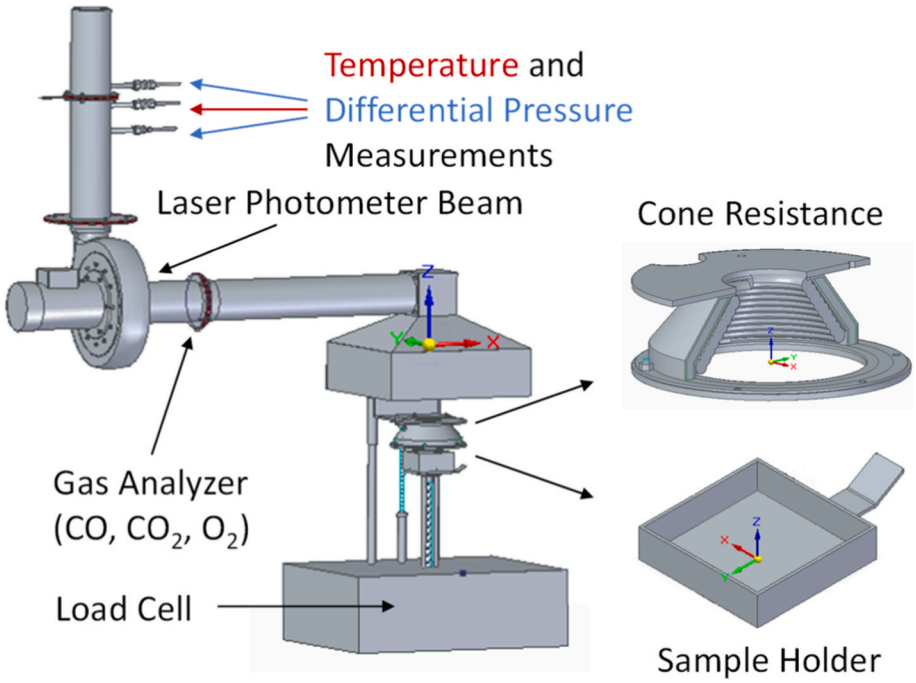

Fig. 3. Schematic representation of cone calorimeter set-up.

of exhaust gas were monitored through thermocouples, smoke sensors, and gas analysers placed in the exhaust gas duct collector. More in detail, a paramagnetic analyser detects oxygen during the test, while an IR analyser identifies the main products of combustion in the gas phase (CO, CO_2). The transient heat release rate (*HRR*) was determined by measuring the oxygen consumption rate in the exhaust gases, following the principle of oxygen consumption calorimetry (Bryant et al., 2012). In addition, a K-type thermocouple (grounded junction, 1 mm diameter) was placed at coordinates 0; 0; 1 cm of the sample holder (Fig. 3), corresponding to the lower layer of the sample, to collect the time evolution of the temperature of the tested materials.

2.5. Assessment of characteristic rates

Based on the collected data and identified chain of events, the characteristic rate of liquefaction ν_{Liq} (Equation (1)), and vapour production ν_{Vap} (Equation (2)), of samples exposed to an external heat flux q, during cone calorimeter tests were assessed.

$$\nu_{Liq} = \frac{q}{\rho_S \cdot \Delta H_{Liq}} \tag{1}$$

$$\nu_{Vap} = \frac{q}{\rho_L \cdot \Delta H_{Vap}} \tag{2}$$

where ρ and ΔH respectively stand for density and latent heat, and the subscripts S and L indicate solid or liquid properties. It is worth noting that ν_{Vap} account for the production of vapour polymers, regardless of the specific series of events occurring. The comparison of dedicated models for evaporation and cracking reactions (e.g., Lee's model (Lee and Lyczkowski, 2000) and the Arrhenius equation) is recommended. The overall reaction rate (ν_{Ov}) was calculated following the definition provided in Equation (3), where MLR is the average mass loss rate computed over the stable burning phase, ρ_S is the density of the solid, and A is the area exposed to the external heat flux.

$$\nu_{Ov} = \frac{MLR}{\rho_S \cdot A} \tag{3}$$

The obtained values were compared to identify the rate-determining step, if present. Besides, the overall exothermicity, experimentally determined in terms of *HRR*, was compared with a numerical value ($\overline{HRR}_{num}$) defined in Equation (4). To this end, TG-MS analysis was first used to identify the species potentially generated during thermal decomposition and to determine their relative distribution. The latter was combined with the specific MLR per unit area measured in the CC tests to quantify the rate of formation of each species (r_i) at the liquid-vapour interface. At this stage, a complete and instantaneous conversion to carbon monoxide and carbon dioxide was considered based on the yields measured by CC. The corresponding heat of reactions (ΔH_{r_i}) were calculated based on the thermodynamic database provided by a high level of theory quantum mechanical calculations and by the National Institute of Standards and Technology (NIST) (Pickard et al., 2005).

$$\overline{HRR}_{num} = \sum_i \left(r_i \cdot \Delta H_{r_i}\right) \tag{4}$$

2.6. Determination of safety parameters

Safety parameters such as the ignition time t_{ig}, thermal response parameter *TRP,* and combustion efficiency *CE* were assessed. The ignition time is intended as the time corresponding to the realisation of a stable flame lasting at least 10 s. The *TRP* was obtained following Equation (5), where $q_{e,i}$ is estimated as the intercept of the curve depicting q against $(1/t_{ig})^{0.5}$. Additional information on the definition of these parameters can be found elsewhere in the literature (Tahmid Islam et al., 2023). *CE* indicates the combustion effectiveness based on the measured volumetric fraction of carbon monoxide (C_{CO}) and carbon dioxide (C_{CO2}), as defined in Equation (6).

$$TRP = 2\, q_{e,i} \sqrt{\frac{t_{ig}}{\pi}} \tag{5}$$

$$CE = \frac{C_{CO_2}}{C_{CO} + C_{CO_2}} \tag{6}$$

The determination of the minimum external flux required to generate a stable flame in the case of a piloted ignition ($q_{\min}$) was also carried out, assuming it as 0.76 $q_{e,i}$ (Tahmid Islam et al., 2023). Bearing

in mind the abovementioned definition, additional tests at external heat flux 1 kW/m^2 lower than the obtained q_{min} were performed for all the investigated mixtures to evaluate the accuracy and validity of the posed assumptions.

3. Results and discussion

3.1. Determination of the chain of events

The measured profiles obtained through DSC analyses for dry polymers are reported in Fig. 4. DSC analyses allowed for the identification of threshold temperatures for the main physico-chemical phenomena involving the analysed species at the investigated conditions, as reported in Table 1. The corresponding enthalpies were also indicated.

Compared to conventional polyolefins (e.g., polyethene and polypropylene), which exhibit sharp and well-defined melting transitions (Menard and Menard, 2016), PHB and PHBV display overlapping melting and early degradation peaks. According to the current literature, the first peak measured during the heating phase can be attributed to melting (Takahashi et al., 2012), whereas the identification of the main phenomena leading to the second peak is controversial, probably attributed to a degradation process initiated from chain scission of the ester linkage (Li et al., 2003). Under the investigated conditions, a pronounced peak, having ΔH_d of 592 J/g, can be observed at a T_d of 300 °C. The absence of a crystallisation peak once 360 °C is reached suggests an almost complete consumption of the investigated materials. Similar thermal behaviour can be observed in PHBV, wherein an analogous peak of ΔH_d of 590 J/g was depicted at T_d equal to 299 °C. To identify the main phenomena occurring at T_d, thermal gravimetric mass spectrometry analysis was performed. The evolution of the mass of the samples with time under a constant heating rate of 10 °C/min is reported in Fig. 5 for all the investigated species. Besides, the list of species, having a molecular weight lower than 100 g/mol, detected at T_d is reported in Table 2.

The increase in temperature up to T_d leads to an abrupt consumption of polymers, which suggests the occurrence of physico-chemical phenomena in the liquid-vapour phase. Indeed, the liquefaction temperatures (T_L) of the investigated polymers are considerably lower than T_d, being ~165 °C. Under these conditions, both PHB and PHBV exhibit a relevant peak at m/z of 86 (Xiang et al., 2016). This peak is attributed to crotonic acid, a major volatile compound generated during the thermal degradation of both polymers. Its prominent and consistent detection at this stage highlights crotonic acid as the possible principal degradation product, indicating its central role in the early decomposition process. Simultaneously, smaller species and radicals are also formed, resulting from the degradation of the polymeric chain. For PHB, the observed radical at this mass could result from the cleavage of the ester linked to carbon-3, producing crotonic acid and shorter polymer fragments. PHBV similarly can fragment at the same cleavage point of PHB, or, due to the complexity of its chemical structure, the cleavage point could involve the breakage of the ester linked to carbon-3 of 3-hydroxy valerate. The α-cleavage reaction resulted in the loss of the alkoxy group from the ester to the corresponding acylium ion and was observed, as testified by the signal at 71 m/z. A second chemical species can be observed for the PHB at 60 m/z, probably due to the loss of the alkyl group from the acyl portion of the ester molecule, which appeared as acetic acid formation. The appearance of a significant m/z value at 69 suggests the breakage of the ester bond, potentially linked to the side chains present in PHB and PHBV; while for crotonic acid, the same signal could be attributed to the loss of the hydroxyl group. The occurrence of this fragmentation pattern underlines the chemical reactivity of crotonic acid under heating conditions and suggests its involvement in secondary decomposition steps.

Other signals (e.g., m/z 45) are possibly related to the loss of the carboxyl group in the molecules as subsequent fragmentations. These

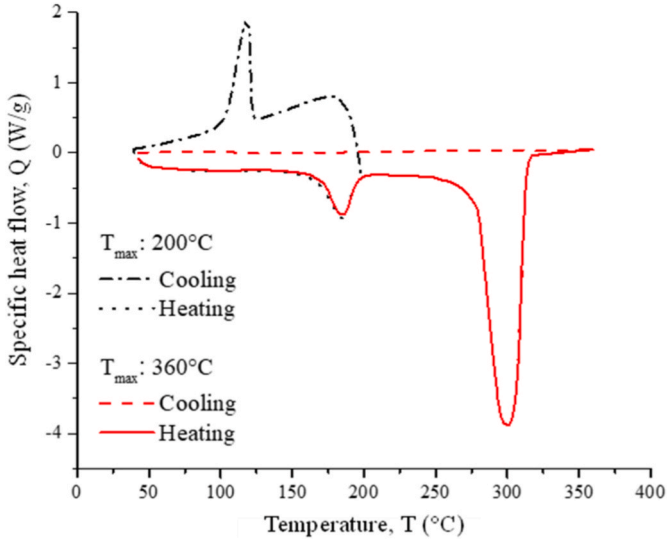

Fig. 4. Heat flow profiles obtained under a heating rate of 10 °C/min up to 200 °C and 360 °C.

Table 1
Crystallisation (T_{cr}, ΔH_{cr}), melting (T_m, ΔH_m), and degradation (T_d, ΔH_d) properties for PHB, PHBV obtained by means of DSC analysis under a heating rate of 10 °C/min.

Species	T_{cr} (°C)	T_m (°C)	T_d (°C)	ΔH_{cr} (J/g)	ΔH_m (J/g)	ΔH_d (J/g)
PHB	118.38	184.72	300	77.75	48.32	592
PHBV	116.76	181.18	299	73.31	47.18	590

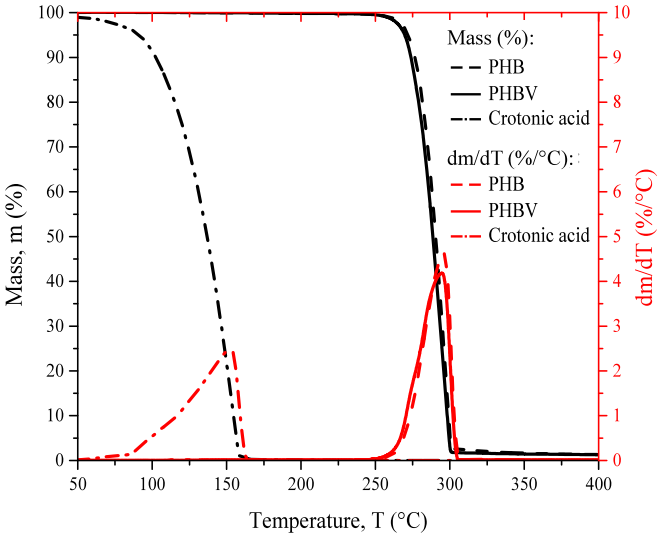

Fig. 5. Mass loss and derivative profiles under 10 °C/min in a nitrogen environment by TG-MS tests.

Table 2
List of species detected by TG-MS tests at T_d under 10 °C/min in a nitrogen environment.

Species	m/z	PHB	PHBV	Crotonic Acid
$C_4H_6O_2$	86	Yes	Yes	Yes
$C_3H_3O_2$	71	Yes	Yes	No
C_4H_5O	69	Yes	Yes	Yes
$C_2H_4O_2$	60	Yes	No	No
COOH	45	Yes	Yes	Yes

observations are in line with the reaction pathways reported in the literature for the thermal decomposition of the most common biopolymers, showing a cleavage reaction (cis-elimination) as the initiation step, followed by a stereoselective cis-elimination, leading to the formation of trans-crotonic acid and its oligomers (Chen et al., 2023). In addition, it is worth noting that crotonic acid represents a common building block within the decomposition of biopolymers (Chen et al., 2023), promoting dedicated investigations on its chemistry and kinetics in either inert or reactive environments. Given its early and abundant formation during the thermal degradation of PHB and PHBV, crotonic acid emerges as a crucial intermediate to be characterised separately. Its specific behaviour, including volatilisation, fragmentation, and possible secondary reactions, could significantly affect the overall decomposition pathways and kinetics of the parent polymers. Therefore, a dedicated experimental focus on crotonic acid is necessary to disentangle its contributions and to improve the reliability of kinetic models. For these reasons, experimental tests were conducted in this work for crotonic acid under the same operative conditions described in the methodological section, as well. Thermogravimetric analysis reveals that PHB and PHBV exhibit mass loss at lower temperatures than conventional polymers such as PE, PP, and PMMA (Conesa et al., 1996; Ferriol et al., 2003), reflecting the expected lower thermal stability of biopolymers. A negligible reduction in mass can be observed at temperatures below T_d once PHB and PHBV are of concern, whereas the mass of crotonic acid is significantly reduced once a temperature of 70 °C is reached. This sharp mass loss at low temperature confirms the high volatility and thermal sensitivity of crotonic acid, supporting the need to investigate its behaviour independently. These experimental observations strongly motivated the dedicated study presented herein, which aims to confirm and quantify the role of crotonic acid within the global thermal decomposition mechanism of PHB and PHBV. For the sake of conciseness, data collected during isothermal tests at T_d are reported in Fig. 6, whereas the homologous data for the remaining temperatures within the range of 300 – 360 °C are included in the supplementary materials.

Before the achievement of the target temperature, a negligible variation in mass was measured. During the isothermal stage, complete consumption is reached in 4 and 3 min for PHB and PHBV, respectively. Noteworthy, an almost constant variation in mass can be observed for PHB and PHBV. Based on the combination of the data collected in this work, this consumption of the initial sample can be attributed to the formation of crotonic acid or the evaporation of intermediate species. In the case of polymers, the transition to the vapour phase may not occur at

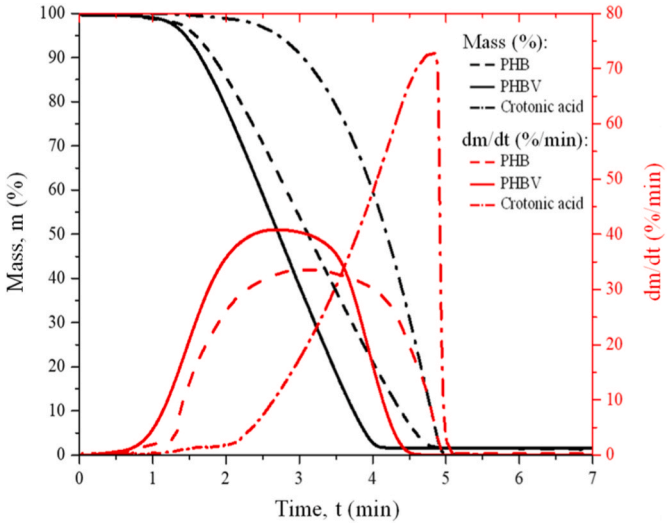

Fig. 6. Weight loss and derivative profiles versus time obtained from isothermal TGA at the temperature of T_d. The reported time starts once T_d is reached.

a well-defined boiling point but rather within a temperature range (T_{NB}), likely due to the complex and heterogeneous molecular structure. The described chain of events characterising the pyrolysis of the investigated mixtures is schematized in Fig. 7.

Once solvent-polymer mixtures are of concern, mass ratios and mixing time can play a significant role in the degradation behaviour. The effects of the mixing time on the results obtained by DSC experiments are reported for two different ratios of PHBV/toluene (i.e., 0.66 and 1). More specifically, the first contact time considered corresponds to a null value (t_0), whereas the second value refers to a contact time representative of steady-state conditions (t_∞). Besides, the enthalpies of the melting (ΔH_m) and degradation (ΔH_d) steps are listed in Table 3 for the reported conditions. Similar data for contact times within t_0 and t_c can be found in the supplementary materials.

Although melting and degradation temperatures are not affected by the initial composition and contact time, both ratios exhibit a slightly higher ΔH_m, compared to pure PHBV, suggesting that toluene may influence the conformational organisation of the polymer, consequently increasing the energy requisites for the processes (Pich et al., 2006a). With increased contact times, a decrease in fusion enthalpy and degradation peak of PHBV is observed. This trend may be attributed to solvent diffusion and polymer swelling at longer contact times, leading to weakened crystallinity and subsequent reductions in reference enthalpies and temperatures (Werker et al., 2023). Moreover, the observed variations in enthalpy are not particularly significant, thus limiting the ability to conclusively support the proposed hypothesis. These observations highlight how small-scale calorimetric analyses may not fully capture the complexity of such mixed systems, especially when involving gradual transitions or concurrent processes. In these conditions, negligible variations may be difficult to address with sufficient clarity, suggesting the need for more representative approaches operating on a larger scale to better resolve overlapping thermal phenomena.

3.2. Evaluation of the thermal behaviour

Proceeding to the investigation of the oxidation mechanism from a bench-scale point of view, attention is directed towards the examination of *HRR* and *MLR* profiles resulting from dry polymer tests under different heat flux conditions, as illustrated in Fig. 8 for PHBV.

PHB and PHBV exhibit peak HRRs comparable to conventional polyolefins, but with lower effective heat of combustion and significantly reduced smoke production, which can be attributed to the influence of their oxygenated backbone on fire behaviour (Quan et al., 2022). Considering the pyrolysis mechanism developed and presented in the previous sections, the chemistry of the vapour phase was assumed as governed by crotonic acid. Hence, the measured *HRRs* were compared with numerical *HRRs* obtained accounting for the conversion of crotonic acid to carbon monoxide (r_1) and the conversion of crotonic acid to carbon dioxide (r_2) only.

$$r_1 : C_4H_6O_2 + \frac{5}{2} O_2 \rightarrow 4\,CO + 3\,H_2O$$

$$r_2 : C_4H_6O_2 + \frac{9}{2} O_2 \rightarrow 4\,CO_2 + 3\,H_2O$$

For the sake of conciseness, additional parameters obtained under a flux of 50 kW/m^2 were reported in Table 4.

Although the presence of an ignition source, both polymers exhibit an almost negligible *HRR* at 7 kW/m^2, as will be discussed in the following section in detail. Conversely, once a radiative flux of 15 kW/m^2 is provided, a stable flame can be observed after 6 min, in the presence of the spark. Afterwards, an almost constant *HRR* was measured until decay was observed after 13 min due to the dearth of fresh material. Analysing the tests providing heat fluxes of 25 kW/m^2 and 35 kW/m^2, samples produced a stable flame starting from 1 to 2 min, respectively. However, only for the latter condition, PHBV

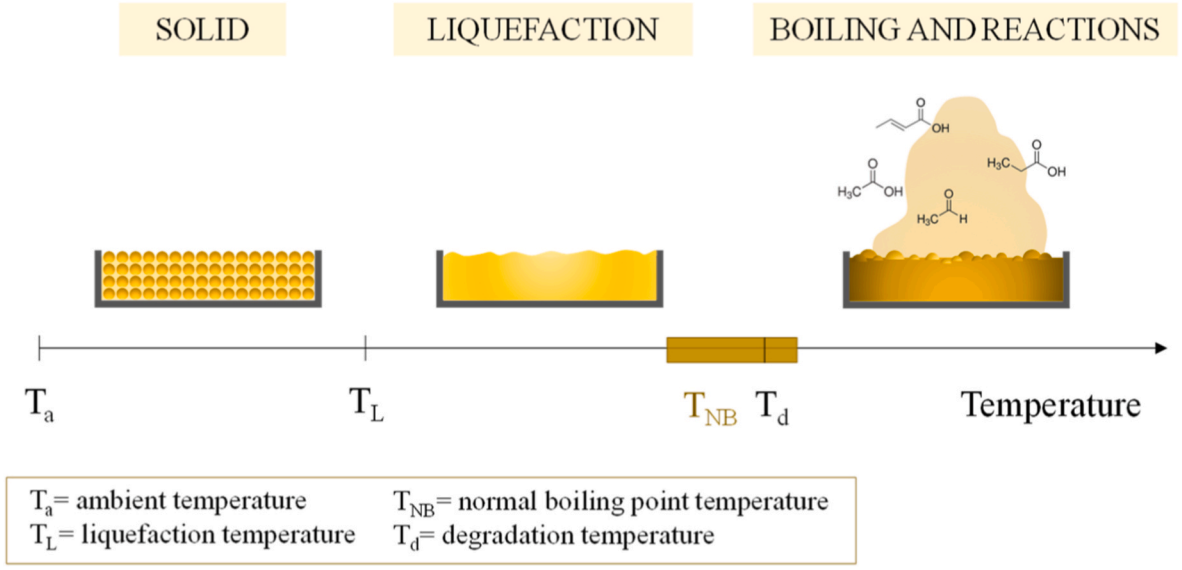

Fig. 7. Schematic representation of the hypothesised mechanistic model for the pyrolysis of PHB and PHBV.

Table 3
Melting (ΔH_m) and degradation (ΔH_d) enthalpies of PHBV/toluene mixtures with different contact times (t_c) compared with a sample of dry PHBV, as obtained by DSC tests having a heating rate of 10 °C/min and a maximum temperature of 360 °C in a nitrogen environment.

Sample	t_c = 0 h		$t_c \to \infty$	
	ΔH_m (J/g)	ΔH_d (J/g)	ΔH_m (J/g)	ΔH_d (J/g)
PHBV/toluene (0.66)	56.46	565.90	52.21	524.60
PHBV/toluene (1.00)	58.01	594.30	52.87	520.00
PHBV	47.18	590.00	-	-

undergoes autoignition, i.e., producing a self-sustained and stable flame without an external ignition source. Increasing the thermal flux to 50 kW/m^2 intensifies this autoignition phenomenon. Hence, PHBV not only sustains oxidation independently but also exhibits increased intensity, as evidenced by the *HRR* profiles. Similar trends can be observed once *MLR*s are analysed. Besides, the conveyed profiles show a moderate increase in *MLR* once the stable flame is observed, suggesting the achievement of a thick layer behaviour, following the definitions reported in the literature (DiDomizio et al., 2021). This trend is more evident at higher external fluxes, possibly because of the increased efficiency in the combustion processes, which has positive feedback on the material consumption. Almost negligible variations can be observed between the data collected at steady-state conditions for the two polymers analysed in this work. However, once the transient regime is of concern, either the peak *HRR* (*pHRR*) or the corresponding time (*tpHRR*) is significantly affected by the initial composition. This observation confirms that only the kinetics of the initial stages (e.g., liquefaction, evaporation, and formation of intermediates) are determined by the chemical structure of the macromolecules, whereas the fate of the intermediates and the kinetics of subsequent phenomena are common between PHB and PHBV degradation. Indeed, the comparison of numerical and experimental *HRR* shows an excellent agreement, confirming the possibility of integrating the pyrolysis mechanism with a detailed kinetic mechanism dedicated to the chemistry of crotonic acid available in the current literature (Wako et al., 2021) to obtain an overall oxidation mechanism for the investigated polymers. Besides, during the experimental tests providing an external heat flux of 15 kW/m^2, temperature profiles were acquired by K-type thermocouples (as reported in supplementary materials), showing a linear increase in temperature up to about 100 °C, which is attributed to sample drying, followed by a steeper increase until the melting temperature is reached. Then, a constant temperature profile is measured. Eventually, a further increase up to a maximum temperature of 277 °C and 257 °C was measured for PHB and PHBV before the ignition, respectively. Similar

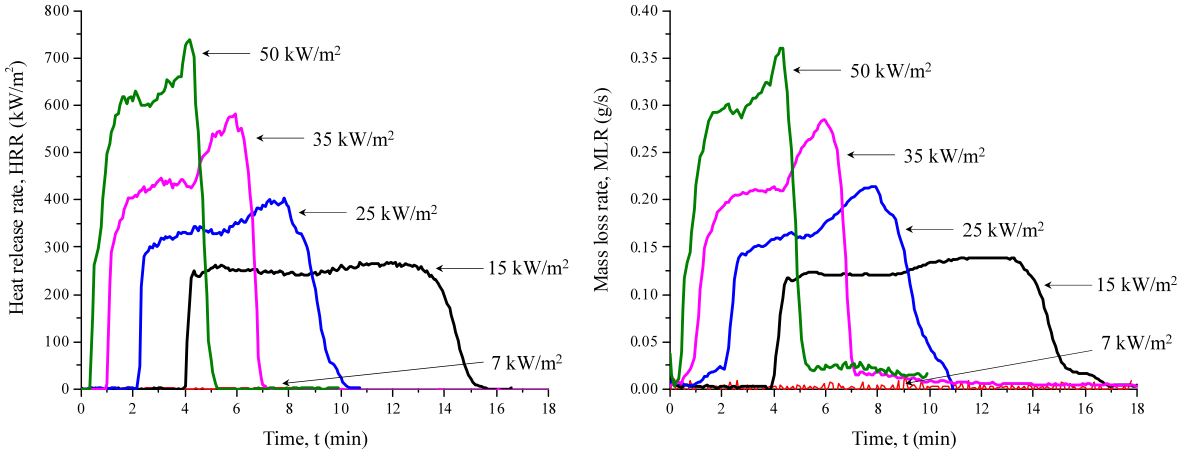

Fig. 8. Heat release rate (left) and Mass Loss Rate (right) profiles of PHBV under different thermal flux conditions (i.e., 7, 15, 25, 35, and 50 kW/m^2).

Table 4
Parameters obtained via cone calorimeter at 50 kW/m^2, including both steady-state and peak values. Steady state: *EHC*, Effective Heat of Combustion; *MLR*, Mass Loss Rate; *COY*, CO yield; CO_2Y, CO_2 yield; $\overline{HRR}_{exp}$, Experimental Heat Release Rate; $\overline{HRR}_{num}$, Numerical Heat Release Rate. Peak values: *pHRR*, peak of the Heat Release Rate; *tpHRR*, time of pHRR; t_{ai}: time of autoignition.

	PHB	PHBV
pHRR (kW/m^2)	817	740
EHC (MJ/kg)	21.4	21.2
MLR (g/s)	0.306	0.309
COY (kg/kg)	0.011	0.012
CO_2Y (kg/kg)	1.74	1.77
tpHRR (s)	265	250
t_{ai} (s)	15	20
$\overline{HRR}_{exp}$ (kW)	6.05	5.85
$\overline{HRR}_{num}$ (kW)	5.62	5.60

Table 5
Parameters obtained by cone calorimeter tests of different PHBV/toluene ratios at 25 kW/m^2 *pHRR*: peak of heat release rate; *tpHRR*: time to peak of heat release rate; *pMLR*: peak of mass loss rate; t_{ss}: time step of quasi-steady state phase.

PHBV/toluene	*pHRR* (kW/m^2)	*tpHRR* (s)	*pMLR* (g/s)
Pure toluene	2574	90	0.684
0.66	2384	30	-
1.00	1980	30	0.579
1.50	2329	60	0.598
3.00	876	110	0.425
PHBV/toluene	*HRR* (kW/m^2)	t_{ss} (s)	*MLR* (g/s)
Pure PHBV	433	160	0.219
0.66	406	90	0.220
1.00	468	100	0.221
1.50	446	155	0.206
3.00	417	175	0.198

trends were observed for the other cases, although slightly higher temperatures were measured at each step, in line with the hypothesised mechanism. Fig. 9 reports the time evolution of *HRR* and *MLR* of a PHBV/toluene mixture with a 1:1 wt ratio under different external heat fluxes. Similar data are reported in the supplementary materials for the remaining species and mixtures investigated in this work.

Once wet polymers are considered, a stable flame is established only after a peak in *HRR* and *MLR* is observed. Notably, referring to the profiles of pure compounds, it is evident that the contributions from solid and liquid samples are readily distinguishable in the investigated mixtures. Indeed, the *HRR* and *MLR* profiles of toluene-containing mixtures exhibit rapid development and reach notably high values in shorter timescales, reflecting the volatility and flammability of this solvent. Conversely, the *HRR* and *MLR* profiles of mixtures containing PHBV or PHB display a moderate trend, characterised by a nearly stationary phase, indicative of its comparatively slower combustion kinetics. The profiles resulting from the investigated mixtures represent the combination of their respective contributions, suggesting that the relative contributions of the two components are distinguishable by a valley separating the two distinct profiles of *HRR* and *MLR*, regardless of the external flux. Increasing the external flux, the rapid heating promotes faster thermal degradation, resulting in a more distinct separation between the oxidation profiles of toluene and PHBV. This observation is in line with the assumption of a first peak dominated by toluene and a second peak ruled by the degradation of PHBV. For these reasons, Table 5 reports the main parameters derived from the CC, distinguishing the contributions of the liquid solvent and the solid for each blend of PHBV/toluene. More specifically, the peak in heat release rate (*pHRR*), the corresponding time (*tpHRR*) and the peak of the mass loss rate (*pMLR*) are delineated for the transient phase, whereas the steady state value of *HRR* and *MLR*, together with the duration of the steady state (t_{ss}), were considered for the stable phase.

As a highly volatile solvent, toluene showcases notably high peak heat release rates (*pHRR*) across all concentrations, reaching a maximum value of 2574 kW/m^2 for the pure compound. This propensity for rapid heat release can be attributed to the molecular structure of the liquid, characterised by aromatic hydrocarbons that readily undergo exothermic reactions when exposed to heat. Although the presence of distinguished areas attributable to the investigated liquid and solid materials has been observed either for *MLR* or *HRR* profiles, the collected peaks are significantly reduced by the addition of PHBV to toluene, suggesting the existence of synergies and interactions between them during the ignition phase. Conversely, the main parameters describing the quasi-steady state phase are less affected by the initial composition. For these reasons, a specific focus will be given to the evaluation of the ignition behaviour of dry and wet polymers.

3.3. Estimation of the characteristic rates

As reported in Table 6, the comparison of the characteristic rates of phenomena relevant for the degradation of PHB and PHBV at increasing external heat fluxes reveals important insights into the decomposition mechanisms.

The liquefaction rate (v_{Liq}) is consistently one order of magnitude higher than both v_{Vap} and v_{Ov} across all tested conditions, indicating that the melting process occurs rapidly and is not rate-limiting. Conversely, v_{Ov} and v_{Vap} exhibit strikingly similar values for both polymers, particularly at lower heat fluxes, suggesting that vaporisation represents the

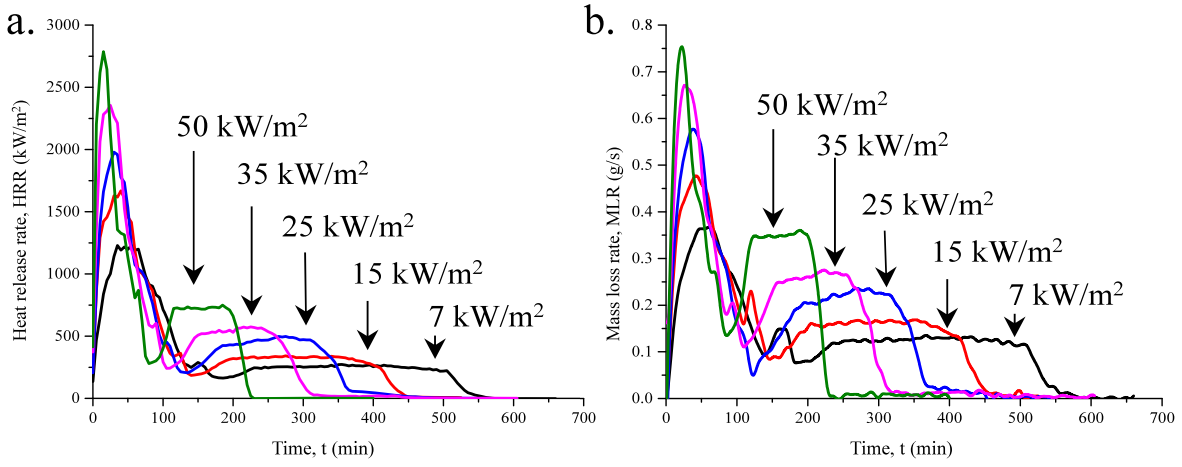

Fig. 9. Heat release rate (a.) and mass loss rate (b.) profiles of PHBV/toluene:1 sample at different heat fluxes (7 – 50 kW/m^2).

Table 6
Characteristic rates of liquefaction (v_{Liq}), vapour production (v_{Vap}), and overall degradation (v_{Ov}) for PHB and PHBV measured at four external heat fluxes (15, 25, 35, and 50 kW/m^2).

	PHB				PHBV			
Heat flux (kW/m^2)	15	25	35	50	15	25	35	50
v_{Ov} (cm/s)	$1.25 \bullet 10^{-3}$	$1.64 \bullet 10^{-3}$	$2.11 \bullet 10^{-3}$	$3.21 \bullet 10^{-3}$	$1.17 \bullet 10^{-3}$	$1.75 \bullet 10^{-3}$	$2.31 \bullet 10^{-3}$	$2.91 \bullet 10^{-3}$
v_{Liq} (cm/s)	$2.48 \bullet 10^{-2}$	$4.14 \bullet 10^{-2}$	$5.79 \bullet 10^{-2}$	$8.28 \bullet 10^{-2}$	$2.54 \bullet 10^{-2}$	$4.24 \bullet 10^{-2}$	$5.93 \bullet 10^{-2}$	$8.48 \bullet 10^{-2}$
v_{Vap} (cm/s)	$2.03 \bullet 10^{-3}$	$3.38 \bullet 10^{-3}$	$4.73 \bullet 10^{-3}$	$6.76 \bullet 10^{-3}$	$2.03 \bullet 10^{-3}$	$3.39 \bullet 10^{-3}$	$4.75 \bullet 10^{-3}$	$6.78 \bullet 10^{-3}$

rate-controlling step in the overall thermal degradation process. This close correspondence implies that the transition from liquid to vapour governs the global mass loss rate, while contributions from processes such as bubbling, charring, or secondary condensed-phase degradation appear negligible under the experimental conditions. In this regime, evaporation could plausibly take place concurrently with the onset of thermal degradation. Once comparing the kinetics of the overall phenomenon, the obtained results indicate that the best-fitting chemical kinetic order is null. Nevertheless, this assumption leads to a normalised square error of 0.29, lower than the one corresponding to Lee's model (i.e., 0.15). Therefore, it is possible to conclude that the evaporation best fits the experimental data and it is the rate-determining step for the production of a vapour cloud under the investigated conditions. In this light, it is worth noting that the average relaxation parameters obtained for all the investigated temperatures were 0.15 cm^3/min and 0.16 cm^3/min for PHB and PHBV, respectively. The discrepancies in these parameters between PHB and PHBV suggest distinctive thermal relaxation behaviours, possibly attributable to variations in molecular structure or composition. The data therefore support a degradation model in which liquefaction occurs promptly upon reaching the softening temperature, followed by a slower vaporisation-driven mass removal that defines the overall decomposition rate. At 35 kW/m^2, PHBV shows a slightly higher v_{Ov} compared to PHB (2.31 vs 2.11 $\times$ 10^{-3} cm/s), despite the v_{Liq} and v_{Vap} being nearly identical. This suggests a more efficient thermal transfer or lower melt viscosity in PHBV, which may facilitate vaporisation and, consequently, mass removal. Moreover, at the highest heat flux of 50 kW/m^2, the rates for both PHB and PHBV converge, implying that, beyond a certain threshold of thermal input, material properties lose their relevance in comparison to the dominant influence of heat flux. These findings reinforce the assumption that vaporisation controls the progression of the entire thermal degradation sequence for both PHB and PHBV for all the investigated conditions. The consistency of the trends and the absence of significant differences in the limiting steps between the two polymers further highlight the dominant role of heat-driven vaporisation under the conditions tested.

3.4. Determination of safety parameters

This section was devoted to the quantification of parameters representative of the ignition and flame behaviour of the investigated materials. To characterise the ignitability of polymers, a first effort was devoted to the identification of the minimum heat flux resulting in a stable flame. Once the protocol proposed by Tahmid Islam et al. (2023) (Tahmid Islam et al., 2023) is applied to the whole set of data collected in this work through the CC, minimum heat fluxes of 5 kW/m^2 and 8 kW/m^2 can be obtained for PHBV and PHB, respectively. However, the absence of stable flames observed once PHBV was exposed to 7 kW/m^2 demonstrates that a linear correlation accounting for all tests cannot provide accurate data for the analysed conditions. Therefore, the application of the mentioned relation was limited to tests showing a thick behaviour (e.g., external fluxes $\geq$25 kW/m^2). Following this assumption, minimum fluxes of 14 kW/m^2 and 13 kW/m^2 were obtained respectively for PHB and PHBV. The validity of the obtained minimum fluxes was tested by exposing the samples to an external flux equal to $q_{\min}$ and ($q_{\min}$ - 1 kW/m^2). Hence, the proposed modification to the protocol proposed by Tahmid Islam et al. (2023) is found suitable for the estimation of the minimum ignition fluxes. Starting from the CO and CO_2 production rate measured by the CC and reported in the supplementary materials, *CE* was assessed, showing values larger than 90 % for all the investigated conditions, meaning that a smouldering mechanism is negligible within the decomposition process. This aspect plays a determining role if compared with traditional polymers, because of the reduced likelihood of causing secondary ignitions attributable to the polymers investigated in this work, as well as the lower toxicity of the produced exhaust gas (Porowski et al., 2023). Additional considerations can be drawn from the comparison of the thermal response parameter (*TRP*) of PHB and PHBV (Table 7).

The values of the reported parameters highlight the similar and moderate thermal behaviours for PHB and PHBV, attributed to enhanced molecular arrangements and effective heat dissipation mechanisms. Referring to the temperature profiles resulting from the investigation of wet polymers, regardless of the composition of the analysed mixture, a distinctive initial phase indicative of the liquid solvent having a parabolic trend ($T = \alpha \cdot t^2$) is discernible. Later, a second contribution related to polymer degradation also emerges in terms of measured temperature. In this case, the temperature profile exhibits a near-linear growth over time. In each profile, a temperature peak is observed due to the consumption of solid material and the exposure of the thermocouple to the flame. The characteristic timescales of the two materials align with the contributions identified through *HRR* analysis. The proportionality coefficient (α) and the averaged dT/dt are reported in Table 8.

Interestingly, as the proportion of PHBV increases in the mixtures, slight differences in α can be noted. In addition, considering the collected values for yields of CO and CO_2, an impact on the gas-phase reactions can be expected for liquid-solid systems. Specifically, the greater the percentage of toluene in the sample increases the greater the tendency for the partial oxidation reaction. Therefore, it is possible to infer that the reactivity of toluene is hindered by an additional limiting step not depending on the concentration of toluene and caused by the presence of solid porous species under the abovementioned conditions. In other words, the increased thermal inertia due to the presence of PHBV inherently poses the conditions for an evaporation-dominated regime, which results in increasing the safety parameters of toluene because of a hampered ignition phenomenon. Once the PHBV/toluene ratio of 3.00 is considered, an abrupt decrease in *pHRR* and *pMLR* can be observed concerning the other investigated mixtures. On the one hand, similar α are collected under these conditions, indicating that the evaporation is slightly affected by the modified initial composition.

Table 7
Thermal response parameter (*TRP*) at various external heat fluxes (*q*) for PHB and PHBV.

	q (kW/m^2)	*TRP* (kWs$^{0.5}$/m^2)
PHB	15	242
	25	137
	35	140
	50	49
PHBV	15	174
	25	123
	35	83
	50	50

Table 8
Quadratic proportionality coefficient (α) and temperature derivative (dT/dt) for PHBV/toluene mixtures.

PHBV/toluene	α (°C/s^2)	dT/dt (°C/s)
Pure toluene	0.0101	-
0.66	0.0072	0.817
1	0.007	0.707
1.5	0.0072	0.648
3	0.0078	0.522
Pure PHBV	-	0.469

Therefore, it is possible to infer that a gas-phase phenomenon is determining the overall reactivity of toluene, i.e., a regime dominated by counter diffusion of toluene can be hypothesised once elevated ratios of PHBV to toluene are considered. Eventually, intermolecular interactions between PHBV and toluene could influence a modulation in the distribution of combustion byproducts, affecting the global kinetics of the process.

4. Conclusions

This work presents an innovative strategy combining small-scale and bench-scale calorimetric tests for the characterisation of microscopic and macroscopic behaviour of solid-liquid mixtures exposed to fire. Within this scope, the cases of PHB, PHBV, and PHBV-toluene mixtures were deeply analysed. The possible effects of interactions between toluene and polymers (PHB, PHBV) were experimentally investigated under different boundary conditions, including different initial compositions and external heat fluxes. Two distinguished regions were observed and attributed to the differences in volatility of the investigated components: a first intense combustion attributed to the toluene chemistry and a second, almost constant, degradation of PHBV. The combination of information gathered by the implemented experimental systems elucidated the chain of events and conditions leading to ignition and characterising the resulting stable flame. The relevance of crotonic acid for the chemistry of the investigated polymers was highlighted. Starting from the collected data, kinetic mechanisms were developed for the pyrolysis and oxidation of dry and wet polymers. The most relevant safety parameters were also determined. In conclusion, on the one hand, the acquired knowledge allows for the optimisation of reactive systems. On the other hand, the collected data on the conditions leading to ignition, thermal response parameters, and flame behaviour can inform and support the identification of effective safety measures to mitigate the effects of flame-related scenarios, the implementation of multicriteria procedures for the material selection, and reduce the likelihood of accidental ignitions, improving overall operational safety.

CRediT authorship contribution statement

Benedetta A. De Liso: Writing – original draft, Investigation, Formal analysis, Data curation. **Gianmaria Pio:** Writing – review & editing, Validation, Supervision, Methodology, Conceptualization. **Ernesto Salzano:** Writing – review & editing, Supervision, Funding acquisition.

Declaration of competing interest

The authors declare that they have no known competing financial interests or personal relationships that could have appeared to influence the work reported in this paper.

Appendix A. Supplementary data

Supplementary data to this article can be found online at https://doi.org/10.1016/j.jlp.2026.105966.

Data availability

Data will be made available on request.

References

Abate, T., Amabile, C., Chianese, S., Musmarra, D., Muñoz, R., 2024. Solubility of poly(3-hydroxybutyrate-co-3-hydroxyvalerate) in sustainable and green solvents: effect of HV content and comparison between experimental results and theoretical prediction. J. Mol. Liq. 393, 123640. https://doi.org/10.1016/j.molliq.2023.123640.

ASTM E1354, 2023. ASTM E1354-23 - Standard Test Method for Heat and Visible Smoke Release Rates for Materials and Products Using an Oxygen Consumption Calorimeter.

Bryant, R., Johnsson, E., Mulholland, G., 2012. Characterizing heat release rate transients. Fire Saf. J. 51, 126–132. https://doi.org/10.1016/j.firesaf.2012.04.002.

Bugler, J., Somers, K.P., Silke, E.J., Curran, H.J., 2015. Revisiting the kinetics and thermodynamics of the low-temperature oxidation pathways of alkanes: a case study of the three pentane isomers. J. Phys. Chem. A 119, 7510–7527. https://doi.org/10.1021/acs.jpca.5b00837.

Chen, Hongmei, Chen, F., Chen, Hui, Liu, H., Chen, L., Yu, L., 2023. Thermal degradation and combustion properties of most popular synthetic biodegradable polymers. Waste Manag. Res. 41, 431–441. https://doi.org/10.1177/0734242X221129054.

Conesa, J.A., Marcilla, A., Font, R., Caballero, J.A., 1996. Thermogravimetric studies on the thermal decomposition of polyethylene. J. Anal. Appl. Pyrolysis 36, 1–15. https://doi.org/10.1016/0165-2370(95)00917-5.

De Liso, B.A., Palma, V., Pio, G., Renda, S., Salzano, E., 2023. Extremely low temperatures for the synthesis of ethylene oxide. Ind. Eng. Chem. Res. 62, 6943–6952. https://doi.org/10.1021/acs.iecr.3c00402.

De Liso, B.A., Pio, G., Salzano, E., 2025. Multicriteria approach to assess the fire behaviour of polymers in electrochemical energy storage. J. Loss Prev. Process. Ind. 94, 105541. https://doi.org/10.1016/j.jlp.2024.105541.

De Liso, B.A., Pio, G., Salzano, E., 2024. Small scale pool fires: the case of toluene. J. Loss Prev. Process. Ind. 92. https://doi.org/10.1016/j.jlp.2024.105430.

DiDomizio, M.J., Ibrahimli, V., Weckman, E.J., 2021. Testing of liquids with the cone calorimeter. Fire Saf. J. 126, 103449. https://doi.org/10.1016/j.firesaf.2021.103449.

Fairweather, M., Woolley, R.M., 2004. First-order conditional moment closure modeling of turbulent, nonpremixed methane flames. Combust. Flame 138, 3–19. https://doi.org/10.1016/j.combustflame.2004.03.001.

Ferriol, M., Gentilhomme, A., Cochez, M., Oget, N., Mieloszynski, J.L., 2003. Thermal degradation of poly(methyl methacrylate) (PMMA): modelling of DTG and TG curves. Polym. Degrad. Stabil. 79, 271–281. https://doi.org/10.1016/S0141-3910(02)00291-4.

Girods, P., Bal, N., Biteau, H., Rein, G., Torero, J.L., 2011. Comparison of pyrolysis behaviour results between the cone calorimeter and the fire propagation apparatus heat sources. Fire Saf. Sci. 889–901. https://doi.org/10.3801/IAFSS.FSS.10-889.

Hong, S.G., Hsu, H.W., Ye, M.T., 2013. Thermal properties and applications of low molecular weight polyhydroxybutyrate. J. Therm. Anal. Calorim. 111, 1243–1250. https://doi.org/10.1007/s10973-012-2503-3.

ISO 5660, 2019. ISO 5660-1: 2019. Reaction-to-fire Tests. Heat Release, Smoke Production and Mass Loss Rate Heat Release Rate (Cone Calorimeter Method) and Smoke Production Rate (Dynamic Measurement).

Koller, M., Mukherjee, A., 2022. A new wave of industrialization of PHA biopolyesters. Bioengineering 9. https://doi.org/10.3390/bioengineering9020074.

Lee, M.Y., Lee, T.S., Park, W.H., 2001. Effect of side chains on the thermal degradation of poly(3-hydroxyalkanoates). Macromol. Chem. Phys. 202, 1257–1261. https://doi.org/10.1002/1521-3935(20010401)202:7<1257::AID-MACP1257>3.0.CO;2-Y.

Lee, W.H., Lyczkowski, R.W., 2000. The basic character of five two-phase flow model equation sets. Int. J. Numer. Methods Fluid. 33, 1075–1098. https://doi.org/10.1002/1097-0363(20000830)33:8<1075::AID-FLD43>3.0.CO;2-5.

Li, S.D., He, J.D., Yu, P.H., Cheung, M.K., 2003. Thermal degradation of poly(3-hydroxybutyrate) and poly(3-hydroxybutyrate-co-3-hydroxyvalerate) as studied by TG, TG-FTIR, and Py-GC/MS. J. Appl. Polym. Sci. 89, 1530–1536. https://doi.org/10.1002/app.12249.

Menard, K., Menard, N., 2016. Thermal analysis of polyethylene. Handb. Ind. Polyethyl. Technol. 217–238. https://doi.org/10.1002/9781119159797.ch6.

Patel, R.J., Wang, Q., 2016. Prediction of properties and modeling fire behavior of polyethylene using cone calorimeter. J. Loss Prev. Process. Ind. 41, 411–418. https://doi.org/10.1016/j.jlp.2015.11.009.

Pich, A., Schiemenz, N., Boyko, V., Adler, H.J.P., 2006a. Thermoreversible gelation of biodegradable polyester (PHBV) in toluene. Polymer (Guildf.) 47, 553–560. https://doi.org/10.1016/j.polymer.2005.11.070.

Pich, A., Schiemenz, N., Corten, C., Adler, H.J.P., 2006b. Preparation of poly(3-hydroxybutyrate-co-3-hydroxyvalerate) (PHBV) particles in O/W emulsion. Polymer (Guildf). 47, 1912–1920. https://doi.org/10.1016/j.polymer.2006.01.038.

Pickard, F.C., Pokon, E.K., Liptak, M.D., Shields, G.C., 2005. Comparison of CBS-QB3, CBS-APNO, G2, and G3 thermochemical predictions with experiment for formation of ionic clusters of hydronium and hydroxide ions complexed with water. J. Chem. Phys. 122, 1–7. https://doi.org/10.1063/1.1811611.

Pio, G., Dong, X., Salzano, E., Green, W.H., 2022. Automatically generated model for light alkene combustion. Combust. Flame 241. https://doi.org/10.1016/j.combustflame.2022.112080.

Porowski, R., Kowalik, R., Ramiączek, P., Bąk-Patyna, P., Stępień, P., Zielecka, M., Popielarczyk, T., Ludynia, A., Chyb, A., Gawdzik, J., 2023. Application assessment of

electrical cables during smoldering and flaming combustion. Appl. Sci. 13. https://doi.org/10.3390/app13063766.
Quan, Y., Zhang, Z., Tanchak, R.N., Wang, Q., 2022. A review on cone calorimeter for assessment of flame-retarded polymer composites. J. Therm. Anal. Calorim. 147, 10209–10234. https://doi.org/10.1007/s10973-022-11279-7.
Ragaert, K., Delva, L., Van Geem, K., 2017. Mechanical and chemical recycling of solid plastic waste. Waste Manag. 69, 24–58. https://doi.org/10.1016/j.wasman.2017.07.044.
Schinazi, G., Price, E.J., Schiraldi, D.A., 2022. Fire testing methods of bio-based flame-retardant polymeric materials. Bio-based Flame-retardant technol. Polym. Mater. 61–95. https://doi.org/10.1016/B978-0-323-90771-2.00009-2.
Srubar, W.V., Wright, Z.C., Tsui, A., Michel, A.T., Billington, S.L., Frank, C.W., 2012. Characterizing the effects of ambient aging on the mechanical and physical properties of two commercially available bacterial thermoplastics. Polym. Degrad. Stabil. 97, 1922–1929. https://doi.org/10.1016/j.polymdegradstab.2012.04.011.
Tahmid Islam, M., Klinger, J.L., Toufiq Reza, M., 2023. Evaluating combustion characteristics and combustion kinetics of corn stover-derived hydrochars by cone calorimeter. Chem. Eng. J. 452. https://doi.org/10.1016/j.cej.2022.139419.
Takahashi, S., Hassler, J.C., Kiran, E., 2012. Melting behavior of biodegradable polyesters in carbon dioxide at high pressures. J. Supercrit. Fluids 72, 278–287. https://doi.org/10.1016/j.supflu.2012.09.009.
Tsampanakis, I., Orbaek White, A., 2021. The mechanics of forming ideal polymer–solvent combinations for open-loop chemical recycling of solvents and plastics. Polymers (Basel) 14, 112. https://doi.org/10.3390/polym14010112.
Vermeer, C.M., Nielsen, M., Eckhardt, V., Hortensius, M., Tamis, J., Picken, S.J., Meesters, G.M.H., Kleerebezem, R., 2022. Systematic solvent screening and selection for polyhydroxyalkanoates (PHBV) recovery from biomass. J. Environ. Chem. Eng. 10, 108573. https://doi.org/10.1016/j.jece.2022.108573.
Wako, F.M., Pio, G., Salzano, E., 2021. Laminar burning velocity and ignition delay time of oxygenated biofuel. Energies 14. https://doi.org/10.3390/en14123562.
Werker, A., Pei, R., Kim, K., Moretto, G., Estevez-Alonso, A., Vermeer, C., Arcos-Hernandez, M., Dijkstra, J., de Vries, E., 2023. Thermal pre-processing before extraction of polyhydroxyalkanoates for molecular weight quality control. Polym. Degrad. Stabil. 209. https://doi.org/10.1016/j.polymdegradstab.2023.110277.
Wu, W., Yermán, L., Hidalgo, J.P., Morrell, J.J., Wiesner, F., 2023. Experimental study on the factors affecting smouldering behaviour of CCA-treated wood. Fire Saf. J. 141. https://doi.org/10.1016/j.firesaf.2023.104003.
Xiang, H., Wen, X., Miu, X., Li, Y., Zhou, Z., Zhu, M., 2016. Thermal depolymerization mechanisms of poly(3-hydroxybutyrate-co-3-hydroxyvalerate). Prog. Nat. Sci. Mater. Int. 26, 58–64. https://doi.org/10.1016/j.pnsc.2016.01.007.
Zhang, Y., Chen, C., 2022. An experimental study on burning characteristics and temperature distribution of inert porous sand bed soaked by leaked combustible liquid. Int. J. Therm. Sci. 179. https://doi.org/10.1016/j.ijthermalsci.2022.107594.